To appear in special issue of Macromolecular Symposia (Wiley VCH in Weinheim) with works presented at the Macromex 2014 conference
To appear 2017

The Solidification Rheology of Amorphous Polymers - Vitrification as Compared to Gelation

H. Henning Winter

Department of Chemical Engineering and Department of Polymer Science and Engineering, University of Massachusetts, Amherst, MA, USA

Summary: Liquid-to-solid transitions of amophous material results from the growth of a heterogeneous, percolating internal structure. The increased connectivity reduces the mobility of internal constituents and dominates the macroscopic rheological properties, which often appear to be very similar for gelation and vitrification. An example near the liquid-to-solid transition is the diverging shear viscosity, which is accompanied by high elasticity and a diverging relaxation time (critical slow down). Gelation and vitrification are hard to distinguish in this way. A distinctive difference, however, was found in the distribution of relaxation modes. Short relaxation modes dominate gelation since most internal constituents maintain their high mobility while, in comparison, the percolating structure is too weak to significantly contribute to the macroscopic behavior. The opposite is found for vitrification, which originates from large, cooperatively-moving regions which finally connect into a percolating structure at the glass transition. As a consequence, the long relaxation modes dominate the approach of the glass transition. Surprisingly, the relaxation time spectrum adopts the same format for both phenomena near the transition, except that the relaxation exponent, *n*, is negative for gelation and positive for vitrification. Mathematically, one is the inverse of the other. The spectrum is cut off by the diverging longest relaxation time. Examples will be shown for these phenomena.

Key Words: gelation, vitrification, critical gel, rheology, polymer

Introduction

Complex fluids are characterized by their elasticity as much as by their viscosity (Pipkin 1982). Elasticity strongly effects the kinematics of flows, especially when they are time-dependent and/or Lagrangian unsteady. Also, elasticity-dominated rheological experiments can help to distinguish complex fluids from one another. A well accepted measure of elasticity is the Deborah number (Reiner 1964), De = τ_{max} / t_{flow} , which compares the longest relaxation time, τ_{max} , of a complex fluid with the time of an imposed deformation or flow, t_{flow}, in a specific application. A large De

indicates strong elastic effects in a given flow. As a consequence of large De, steady state conditions will require long times to develop and cannot be reached anymore in many applications or rheological experiments. Large De rheology has to rely on transient observations at experimental times much shorter than τ_{max}.

This brief communication discusses the linear viscoelasticity of three classes of complex materials, which all belong to the large De species but are fundamentally different in many ways. All three are near their liquid-to-solid transition where high elasticity and a diverging τ_{max} dominate their rheology:

- gelling materials at their transition through the gel point,
- glass forming materials in their approach of the glass transition, and
- polymeric fluids with long linear macromolecules of diverging molecular weight.

At first glance, such different kind of complex materials look very similar. However, linear viscoelastic experiments are able to distinguish the above material groups from one another as will be shown in the following.

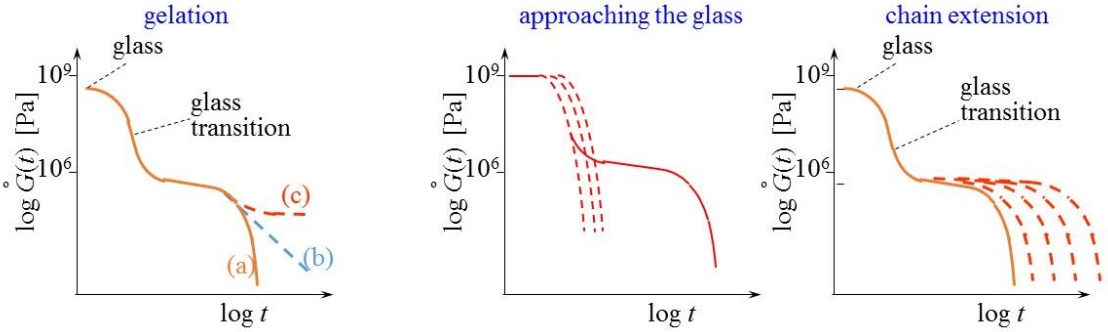

Figure 1: Evolution of the relaxation modulus for gelation (left), approach of the glass transition (middle), and increase of the molar mass of a linear, flexible polymer (right). Gelation rheology is distinctly different before (a) and after (c) the gel point. At the gel point (b), the relaxation modulus diverges and assumes power-law format at long times. For the glassy material, only the approach of the glass transition is shown: the modulus shifts to longer times. This communication focuses on gelation vs glass transition. But for comparison, the increasing molecular size of an entangled polymer is included since its relaxation time spectrum is similar to that of an amorphous material in its approach of the glass. Its relaxation modulus shifts to longer times as the molar mass is increased.

Small amplitude oscillatory shear (SAOS) data, as quantitative measure of linear viscoelastic behavior, can be expressed directly as material functions such as $\tan\delta$, normalized storage modulus

G'/G^*, or normalized loss modulus G''/G^*. Furthermore, SAOS data can be converted into relaxation moduli (schematically shown in Figure 1)

$$G(t) = G_\infty + \int_0^{\tau_{max}} \frac{d\tau}{\tau} H(\tau)\, e^{-t/\tau} \qquad (1),$$

together with their corresponding relaxation time spectra, $H(\tau)$, using the method of Baumgärtel et al. (1989, 1992), for instance. The longest relaxation time, τ_{max}, which belongs to the slowest relaxation process, terminates the relaxation time spectrum in equation 1, $H(\tau) = 0$ for $\tau > \tau_{max}$. A broadly distributed $H(\tau)$ is an expression of the wide range of relaxation processes in materials of broadly distributed internal size scales. The viscoelastic material functions differ distinctly for each of three material groups selected above.

Linear Viscoelasticity of Gelation (or Reverse Gelation)

Gelation and its large effects on molecular dynamics has been a major topic in polymer physics and chemistry (Flory 1953, Miller 1976, De Gennes 1979, Stauffer 1982, Schosseler 1984, Martin 1989, Goldbart 1992, Liu 2006). Many fundamental details are still unknown. Experimental rheology in the vicinity of the gel point showed that, before reaching the gel point and also shortly after having passed through the gel point, the Deborah number assumes large values. Directly at the gel point, the Deborah number diverges, $De \to \infty$, and powerlaw time dependence dominates the relaxation processes (Chambon 1987, Winter 1986a, 1986b). The longest relaxation time diverges so that there is no characteristic time left except for a lower limiting time τ_0. The relaxation modulus and the relaxation time spectrum at the gel point are

$$G_{cg}(t) = G_{cg,0}\,(t/\tau_0)^{-n_{cg}} \quad \text{and} \quad H_{cg}(\tau) = H_{cg,0}(\tau/\tau_0)^{-n_{cg}} \qquad (2)$$

with $0 < n_{cg} < 1$ as exponent, the stiffness $G_{cg,0}$ [Pa] as front factor, and the relaxation strength $H_{cg,0} = G_{cg,0}/\Gamma(n_{cg})$ [Pa] of the broad relaxation time spectrum. Γ is the gamma function. The above spectrum applies to materials at the gel point, called "critical gels" (denoted by subscript cg), and to gelling materials in the immediate vicinity of the gel point. For these, powerlaw scaling is found at long times, $t > \tau_0$, and $\infty > \tau > \tau_0$.

The powerlaw's lower limiting time, τ_0, varies from material to material. Fast relaxation processes with $\tau < \tau_0$, belong to small scale constituents of gelling materials. Their corresponding relaxation time spectrum differs greatly from powerlaw. Fast relaxation modes are interesting by themselves, but discussion of such fast dynamics at $\tau < \tau_0$ would exceed this brief communication by far.

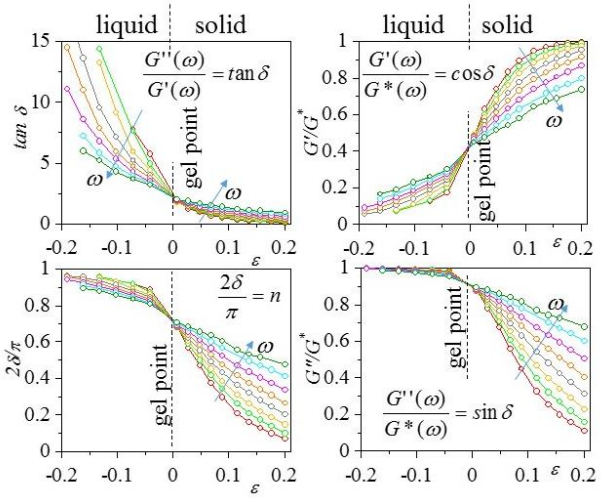

Figure 2: Gel point detection with time-resolved SAOS. The data set of Adolf and Martin (1990) is plotted in four different ways. Material functions are plotted over distance from the gel point, ε, with frequency as parameter. It is essential to alternate SAOS between many frequencies while the gelation process advances. Because of the powerlaw relaxation spectrum at the gel point, all of these material functions become frequency independent at the gel point. These are just examples. Many other material functions would also show frequency independence at the gel point.

The dominance of the power-law spectrum at the gel point has conveniently served for gel point detection through SAOS experiments. Figure 2 compares various linear viscoelastic material functions, all belonging to the same SAOS data set which has been taken from the literature (Adolf and Martin 1990). Gel point detection is made easy due to the appearance of the powerlaw relaxation time spectrum selectively at the gel point, which causes many material functions to become frequency-independent at the gel point. Examples are the frequency-independent tan $\delta(\omega)$, $2\,\delta(\omega)/\pi$, $\sin\delta(\omega)$, $\cos\delta(\omega)$, $G'(\omega)/G^*(\omega)$, $G''(\omega)/G^*(\omega)$, $1/\tan\delta(\omega)$, $\cot\delta(\omega)$, $\tan^2\delta(\omega)$, $\sin^2\delta(\omega)$, $\cos^2\delta(\omega)$ and many more. Most popular for gel point detection is the frequency-independence of $\tan\delta(\omega)$ (Holly 1988). Recently, McKenzie (2016) used $\cos^2\delta(\omega)$ - data to express the transition through the gel point. There is merit in expressing rheological data by means

of a range of material functions. Different material functions of gelation show different sensitivity, some are more frequency dependent before the gel point (tan $\delta(\omega)$, for instance) and some as more frequency dependent beyond the gel point (cos $\delta(\omega)$, for instance). But they all intersect at the gel point as shown in figure 2.

Linear Viscoelasticity in the Approach of the Glass Transition (Soft Glassy Dynamics)

For glass forming liquids in their approach of the glass transition, relaxation processes are typically grouped in two relaxation modes, the α -mode for the long-range connectivity and the β -mode for the small-scale dynamics. The characteristic relaxation times are much larger for the α - than the β -relaxation process. The α -process with its longest relaxation time, $\tau_{\max} = \tau_\alpha$, dominates the long-time viscoelasticity. Here we focus on the α -process.

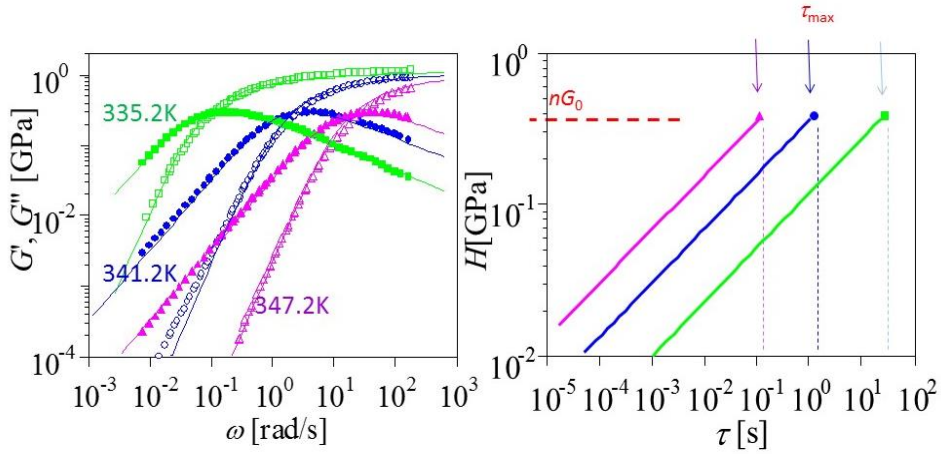

Figure 3: Material functions of a low molecular weight glass former (sucrose benzoate) in the approach of the glass transition: (left) SAOS data McKenna et al. (Hutcheson 2008. Xu 2011), (right) Relaxation time spectra for expressing the SAOS data. The spectra are cut off by the longest relaxation time of their α–process, τ_α .

As the longest relaxation time, τ_α , diverges in the approach of the glass, the α –mode adopts a power-law relaxation time spectrum with positive exponent n_α (Siebenbürger 2009, Winter 2009)

$$H_\alpha(\tau) = H_{\alpha,0}(\tau/\tau_\alpha)^{n_\alpha} \qquad \text{for} \quad \tau \le \tau_\alpha \qquad (3),$$

which is cut off at τ_α. The characteristic shapes of relaxation modulus and the relaxation time spectrum do not change in the approach of the glass (Menon 1996, Hutcheson 2008, Siebenbürger 2009, Pogodina 2011, Xu 2011). They only shift to longer times, see Figure 3. Even at far distance from the glass transition, the relaxation pattern is already fully developed! The only change is seen in the longest relaxation time, which adopts larger and larger values with shrinking distance to the glass.

Little experimental data is available for the soft glass beyond the glass transition since equilibrium states are hard to achieve due to the slow aging processes of the glass. The discussion of this communication is limited to the α-process in the approach of the glass but not beyond.

Linear Viscoelasticity of Polymer Fluids of High Molar Mass

The relaxation time spectrum of long linear flexible chain molecules of uniform length (LLFCMUL) resembles that of soft glassy polymers and is included here for discussion purposes. LLFCMUL do not really undergo a liquid-to-solid transition by molar mass increase, but one might envision an infinitely large molar mass and that the longest relaxation time diverges in this way. The diverging longest relaxation time

$$\tau_{\max} \approx M_W^{3.4}$$

increases with the molar mass, M_W (Graessley 1974, Ferry 1980, Doi 1986, Milner 1998). LLFCMUL relax with a distinct relaxation time spectrum which is closely matched by Baumgärtel -Schausberger-Winter (BSW) spectrum. Baumgärtel et al. (1990) proposed to represent the LLFCMUL spectrum as linear superposition of two modes, the fast mode for the segmental dynamics and the slow mode for the long linear flexible chains and their entanglements. When the molar mass increases, the slow mode becomes stronger and even slower while the fast mode remains nearly unchanged.

The slow mode of the BSW spectrum, $H_{BSW}(\tau)$, represents the entanglement and flow region of the relaxation time spectrum. It has the same format as the alpha mode near the glass transition, eq. 3. $H_{BSW}(\tau)$ adopts the shape of a power-law with positive exponent n_{BSW}

$$H_{BSW}(\tau) = H_{BSW,0}\left(\tau/\tau_{\max}\right)^{n_{BSW}} \qquad \text{for} \quad \tau \le \tau_{\max} \qquad (4).$$

$H_{BSW}(\tau)$ is cut off at $\tau_{\max}$. The positive exponent, n_{BSW}, has known values between 0.2 and 0.3. The relaxation strength, $H_{BSW,0}$, is a material-specific parameter, which depends on the chain flexibility and internal friction of individual polymers (Jackson 1994).

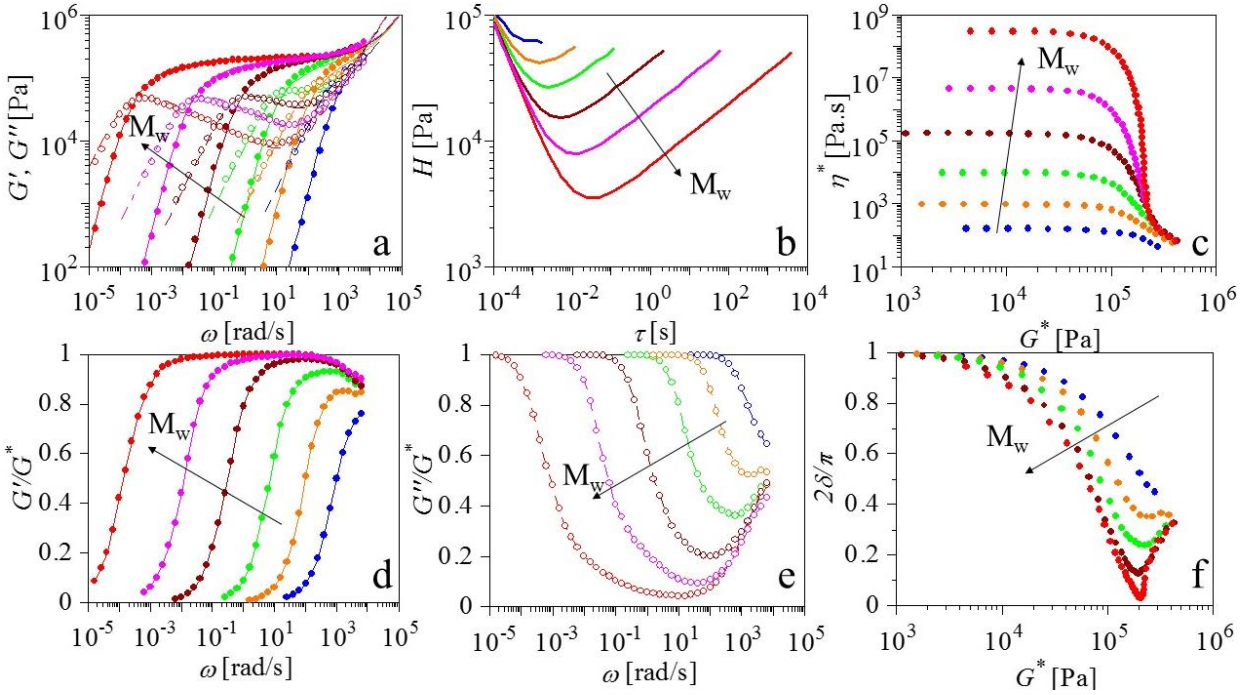

Figure 5: SAOS data of a set of model polystyrenes (Schausberger 1985) at 180°C and the corresponding relaxation time spectra which represent the lines that were drawn through the SAOS data on the left side figure. (a) SAOS data and fit with BSW spectrum, (b) BSW spectra, (c) complex viscosity over G* (stress equivalent), (d) normalized storage modulus, (e) normalized loss modulus, (f) Booij-Palmen plot. All plots belong to the same SAOS data set.

The LLFCMUL spectrum shifts to longer and longer times as the molar mass increases, but it maintains its shape. The constancy of shape is quite remarkable. Even at fairly small molecular weights, the relaxation pattern is already fully developed ! The only change is seen in the longest relaxation time, which adopts larger and larger values as the molecular weight diverges.

Discussion

The relaxation time spectrum $H(\tau)$ quantitatively expresses the relaxation modes of a complex material, their strengths and their characteristic times. The spectrum broadens in the approach of a liquid-to-solid transition. Extremely slow relaxation modes ($\mathrm{De} \to \infty$) govern materials near a

transition state and, for practical reasons, only intermediate modes are accessible to rheological testing. However, already intermediate modes (intermediate characteristic times) assume distinct patterns that can be used to differentiate between gelation and glass transition. *Gelation rheology*, for instance, results in a distinct powerlaw distribution of relaxation modes when the materials reaches its gel point ("critical gel" state). The long-range connectivity in the critical gel is barely established and the slowest relaxation modes are so weak that they hardly contribute at all to the stress. Fast modes have higher probability than slow modes and dominate the stress. The powerlaw relaxation behavior of gelation is limited to a narrow neighborhood of the gel point.

The powerlaw relaxation of the critical gel, however, is not unique. Besides critical gels, there are other viscoelastic materials with several decades of powerlaw relaxation. For example, powerlaw relaxation behavior was found for gluten dough (Tanner 2008, Trevor 2008, 2011), for bottlebrush polymers (Hu 2011, López-Barrón 2015, Daniel 2015, Dalsin 2015), and for branched polyethylene (Wood-Adams 2000, García-Franco 2001).

Different from gelation, the distinct relaxation pattern of the *glass transition* shows up already at far distance from the glass. Relaxation modes arrange in a powerlaw pattern, just as in gelation, but with a positive exponent n_α instead (the powerlaw of gelation has a negative exponent as shown above). The spectrum is cut off at the longest relaxation times, which diverges when the material reaches the glass state. The positive slope of the powerlaw suggests that the slow modes are the largest contributors to the stress as compared to the less important fast modes (inverse behavior to gelation).

The sharp cut-off of the α -spectrum, eq. (3), and the BSW spectrum, eq. (4), seems to represent ideal material behavior. A broadening of the molar mass distribution of LLFCMUL results in a broadening of the cutoff (Baumgärtel 1992) and a broadened glass transition causes the cutoff to broaden for the α -spectrum (Zaccone 2014, Dannert 2014, Laukkanen 2016). A stretched exponential cutoff

$$H_\alpha(\tau) = H_{\alpha,0}\left(\frac{\tau}{\tau_\alpha}\right)^{n_\alpha} \exp\left(-\left(\frac{\tau}{\tau_\alpha}\right)^{\beta}\right) \quad \text{for } \beta<1 \text{ and } n_\alpha \geq 0 \qquad (5),$$

has been used successfully to accommodate the broadening of the transition.

Conclusions

Material-specific linear viscoelasticity of complex fluids provides a frame work for distinguishing gels from glass forming materials (including soft glasses). Much insight was gained by expressing SAOS data in a rich variety of material functions (Ferry 1980) which has become practical with the advent of cyber infrastructure tools (Winter 2006).

Acknowledgement

The study has been supported by a grant from the National Science Foundation (NSF – CMMI 1334460). Data analysis was performed with the IRIS Rheo-Hub software (http://rheology.tripod.com/TOP_P.htm).

References

Adolf D, Martin JE (1990) Macromol 23: 3700
Baumgärtel M, Schausberger A, Winter HH (1990) Rheol Acta 29:400-408
Baumgärtel M, Winter HH (1989) Rheol Acta 28:511–519
Baumgärtel M, Winter HH (1992) J Non-Newt Fluid Mech 44:15-36
Chambon F, Winter HH (1987) J Rheology 31:683-697
Dalsin SJ, Hillmyer MA, Bates FS (2015) Macromol 48:4680–4691.
Daniel WFM, Burdyńska J, Vatankhah-Varnoosfaderani M, Matyjaszewski K, Paturej J, Rubinstein M, Dobrynin AV, Sheiko SS (2015) Nature Materials 15:183-189.
Dannert R, Sanctuary R, Thomassey M, Elens P, Krüger JK, Baller J (2014) Rheol Acta 53:715
de Gennes PG (1979) "*Scaling concepts in polymer physics*". Cornell, Ithaca, New York
Doi M, Edwards S (1986) "*The theory of polymer dynamics.*" Clarendon Press, Oxford
Ferry JD (1980) "*Viscoelastic properties of polymers*," 3rd edn.Wiley, New York
Flory PJ (1953) "*Principles of polymer chemistry*." Cornell University Press, Ithaca, New York
García-Franco CA, Srinivas S. Lohse DJ, Brant P (2001) Macromol 34:3115–3117
Goldbart P, Goldenfeld N (1992) Phys Rev A 45: R5343
Graessley WW (1974) Adv Polym Sci 16, Springer Verlag, Heidelberg
Holly EE, Venkataraman SK, Chambon F, Winter HH (1988) J Non-Newt Fluid Mech 27:17-26
Hu M, Xia Y, McKenna GB, Kornfield JA, Grubbs RH (2011) Macromol 44:6935–6943.
Hutcheson A, McKenna GBJ (2008) J Chem Phys 129:074502
Jackson JK, De Rosa ME, Winter HH (1994) Macromol 27:2426-2431
Laukkanen OV, Winter HH, Soenen H, Seppälä1 J (2016) Proc of the Nodic Soc Rheol 2016.
Liu R, Gao X, Oppermann W (2006) Polymer 47:8488-8494
López-Barrón CR, Brant P, Eberle APR, Crowther DJ (2015) J Rheol 59:865–883.
Martin JE, Adolf D, Wilcoxon JP (1989) Phys Rev A 39: 1325
McKenzie R, Vlassopoulos D (2016) J Rheol 60:367
Menon N, Nagel SR, Venerus DC (1996) Phys Rev Lett 76:1554
Miller DR, Macosko CW (1976) Macromol 9: 206
Milner ST, McLeish TCB (1998) Phys Rev Lett 81:725-728.

Pipkin AC (1986) "*Lectures on viscoelasticity theory*," 2nd edn. Springer, Heidelberg
Pogodina NV, Nowak M, Läuger J, Klein CO, Wilhelm M, Friedrich C (2011) J Rheol 55:241
Reiner M (1964) Phys Today 17: 62
Schausberger A, Schindlauer G, Janeschitz-Kriegl H (1985) Rheol Acta 24:220
Schosseler S, Leibler L (1984) Physique Lett 45: 501
Siebenbürger M, Hajnal D, Henrich O, Fuchs M, Winter HH, Ballauff M (2009) J Rheol 53:707-720
Stauffer D, Coniglio A, Adam A (1982) Adv Polym Sci 44: 103
Tanner R, Qi F, Dai S (2008) J Non-Newt Fluid Mech 148:33-40
Trevor SK, Ng K, McKinley GH (2008) J Rheol 52:417
Trevor SK, Ng K, McKinley GH, Ewoldt RH (2011) J Rheol 55:627
Winter HH (2013) Macromol 46:2425−2432
Winter HH, Chambon F (1986a) J Rheology 30:367-382
Winter HH, Chambon F (1986b) Proc Bi-annual Meet Polym Networks Group, Elsinore, Danmark